Progress In Electromagnetics Research B, Vol. 55, 365–382, 2013

AN ITERATIVE APPROACH FOR THE SYNTHESIS OF OPTIMIZED SPARSE TIME-MODULATED LINEAR ARRAYS

Paolo Rocca[1, *], Michele D'Urso[2], and Lorenzo Poli[1]

[1]ELEDIA Research Center, Department of Information Engineering and Computer Science, University of Trento, Via Sommarive 5, Trento 38123, Italy

[2]SELEX-ES, Via Circumvallazione Esterna di Napoli, Zona ASI, Giugliano (Napoli) I-38100, Italy

Abstract—In this paper, the synthesis of sparse time-modulated linear arrays with minimum number of elements and controlled harmonic radiations is investigated. The proposed iterative approach based on a particle swarm optimization is aimed at finding the array configuration with the minimum number of elements and the optimal pulse sequence that affords a beam pattern with the same features of a reference one also limiting the amount of sideband radiations under a specific threshold. A set of representative numerical examples is discussed to assess the effectiveness and the reliability of the proposed approach.

1. INTRODUCTION

A time-modulated array (TMA) is an antenna device whose elements are excited through periodical waveforms of arbitrary shapes [1] generally realized by means of a set of RF switches [2] inserted in the feed network [3]. Such an architectural solution gives the system a high reconfigurability thanks to the possibility to drive the RF switches with simple digital signals, but it causes the generation of spurious and undesired harmonic signals [the so called sideband radiation, (SR)] due to the periodic time-varying excitations.

In the last decade, after the pioneer work [4] where Yang et al. showed that global optimization algorithms can be profitably applied

Received 28 July 2013, Accepted 10 October 2013, Scheduled 21 October 2013

* Corresponding author: Paolo Rocca (paolo.rocca@disi.unitn.it).

to synthesize time-modulated linear arrays, a great attention has been devoted to suppress spurious harmonic signals. Toward this end, many techniques have been proposed based on differential evolution (DE) [4–7], simulated annealing (SA) [8], and particle swarm optimizer (PSO) [9–11] aimed at minimizing the sideband level (SBL) [4], namely the peak level of the harmonic patterns, or the overall harmonic content [9] or both [11] by suitably defining the time-pulse durations. The possibility to modify the periodic waveforms has been also examined in [12–15] to achieve a better handling of the SRs. More specifically, a simple time-shift between the pulses has been exploited in [12] to control the harmonic patterns, while in [14] splitting rectangular pulses in multiple sub-pulses has been proposed to set the distribution of the sideband power of the harmonic frequencies. Moreover, the use of alternative waveforms (e.g., trapezoidal and raised-cosine) in [15] provided a reduction of the radiated harmonic content. The application of the previous techniques to real-element arrays has been also assessed [16, 17].

Jointly to the minimization of power losses due to SRs, the simplification of the array geometry/architecture of TMAs has been investigated, as well. Thinning strategies aimed at reducing the number of elements have been proposed in [18, 19] and sub-arraying techniques for simplifying the complexity of the feeding network have been studied in [20, 21]. Although the reduction of the radiating elements in equally-spaced time-modulated linear arrays ($TMLA$s) has been already studied in [18] as well as the exploitation of the positions of the array elements as additional degrees-of-freedom of the synthesis process [22], the synthesis of sparse TMAs with minimum number of elements placed in arbitrary locations has not yet been deeply investigated. As a matter of fact, the design of sparse TMAs has been carried out in [22, 23] while the SRs have been optimized through the minimization of the SBL analyzed for the first harmonic pattern.

Concerning the synthesis of sparse arrays, it has been a topic of growing interest in the state-of-the-art literature on standard phased arrays and many techniques have been proposed. Let us consider as representative examples, the matrix pencil method [24], compressive sensing-based techniques [25–27], and convex optimization-based techniques [28, 29]. In principle, such strategies could be applied to also deal with sparse TMAs, but they are not naturally conceived to handle SRs.

In this paper and unlike [22, 23, 30] where the number of array elements was an input parameter of the synthesis process, the proposed strategy is aimed at synthesizing a sparse array with the smallest number of elements affording a beam pattern close to a reference one

at the carrier frequency, while minimizing the amount of sideband power under a user-defined threshold. The optimization is carried out by means the *PSO* [31], namely a stochastic global optimization algorithm able to effectively deal with non-convex (i.e., multi-minima) cost functions as well as real-valued unknowns as needed for the synthesis problems at hand.

The outline of the paper is as follows. The mathematical theory of *TMA*s is summarized in Section 2, whereas the optimization procedure for the synthesis of sparse time-modulated arrangements is described in Section 3. Representative numerical results concerned with state-of-the-art benchmarks and comparisons are presented in Section 4. Finally, some conclusions are drawn (Section 5).

2. MATHEMATICAL BACKGROUND

Let us consider an array of N elements displaced along the z-axis and modulated in time by periodic rectangular waveforms. The arising time-varying array factor turns out to be expressed as the summation of the contribution of each array element as follows

$$\Im(\theta, t) = e^{j2\pi ft} \sum_{n=0}^{N-1} I_n(t) e^{jkz_n \cos(\theta)} \tag{1}$$

where $f \triangleq \frac{1}{T}$ is the working frequency, $k = \frac{2\pi f}{c}$ the wavenumber, c the speed of light, $I_n(t) = I_n U_n(t)$, I_n being the n-th complex static excitation, and $U_n(t)$ models the periodically-repeated rectangular pulsed waveform at the n-th array element [$U_n(t) = U_n(t + mT_p)$, $T_p \triangleq \frac{1}{f_p}$ being the modulation period and $m \in \mathbb{Z}$]

$$U_n(t) = \begin{cases} 1, & t_n^{rise} \leq t \leq t_n^{fall} \\ 0, & \text{otherwise.} \end{cases} \tag{2}$$

By considering the Fourier expansion, the n-th time-varying excitation becomes

$$I_n(t) = I_n \sum_{h=-\infty}^{+\infty} C_{nh} e^{jh2\pi f_p t} \tag{3}$$

where the h-th harmonic term of the the n-th excitation, C_{nh}, is given by

$$C_{nh} = \frac{1}{T_p} \int_{t_n^{rise}}^{t_n^{fall}} U_n(t) e^{-jh2\pi f_p t} = \tau_n \text{sinc}\left(\pi h \tau_n\right) e^{-j\pi h\left(\tau_n + 2\tau_n^{rise}\right)}$$

$\tau_n = \frac{(t_n^{fall} - t_n^{rise})}{T_p}$ $(n = 1, \ldots, N)$ being the normalized n-th switch-on pulse duration, while $\tau_n^{rise} = \frac{t_n^{rise}}{T_p}$ $(n = 1, \ldots, N)$ is the normalized switch-on instant.

By substituting (3) in (1), one obtains the following array factor expressed as the summation of infinite "array factor terms" each one associated to a different h-th harmonic frequency

$$F(\theta) = \sum_{h=-\infty}^{+\infty} F_h(\theta) = \sum_{h=-\infty}^{+\infty} e^{j2\pi(f+hf_p)t} \sum_{n=0}^{N-1} I_n C_{nh} e^{jkz_n \cos(\theta)}. \quad (4)$$

At the carrier frequency ($h = 0$), the corresponding array factor term turns out to be

$$F_0(\theta) = \sum_{n=0}^{N-1} I_n \tau_n e^{jkz_n \cos(\theta)}. \quad (5)$$

Although such a contribution can be theoretically isolated by means of a suitable filtering, the other harmonic terms in (4) still represent a waste of power to be properly handled. Such a power loss is equal to [32, 33]

$$P_{SR} = \sum_{n=0}^{N-1} \left[|I_n|^2 \tau_n (1 - \tau_n) \right] + 2 \sum_{n=0}^{N-2} \sum_{m=n+1}^{N-1} \mathrm{Re}\{I_n I_m^*\} \mathrm{sinc}[k(z_n - z_{:m})] (\widetilde{\tau}_{nm} - \tau_n \tau_m) \quad (6)$$

where $\widetilde{\tau}_{nm}$ denotes the portion of the modulation period in which the n-th and the m-th array elements are in the 'on' state. For convenience, we usually consider the percentage of SR over the total radiation,

$$SR = \frac{P_{SR}}{P_{tot}} = \frac{P_{SR}}{P_{CF} + P_{SR}} \quad (7)$$

instead of P_{SR}, P_{CF} being the power radiated at the working frequency [32] given by

$$P_{CF} = \sum_{n=0}^{N-1} (|I_n| \tau_n)^2 + 2 \sum_{n=0}^{N-2} \sum_{m=n+1}^{N-1} \mathrm{Re}\{I_n I_m^*\} \tau_n \tau_m \mathrm{sinc}[k(z_n - z_m)]. \quad (8)$$

3. ITERATIVE OPTIMIZATION APPROACH

The synthesis problem at hand then consists in affording a radiated pattern matching a reference one, while controlling the amount of

sideband radiation by setting the optimal pulse sequence, $\underline{\tau} = \{\tau_n;\ n = 0, \ldots, N_{opt} - 1\}$, and the locations, $\underline{d} = \{d_n = (z_{n+1} - z_n);\ n = 0, \ldots, N_{opt} - 2\}$, of the minimum (N_{opt}) number of array elements within a prescribed aperture length, L_{ref}.

Towards this end, the following iterative (υ being the iteration index) procedure has been implemented (Fig. 1):

- **Step 1** — *Initialization* $(\upsilon = 1)$:
  (a) Choice of the reference array/pattern and definition of the target parameters for the array geometry and the pattern masks: N_{ref} and L_{ref} being the number of array elements of the reference array and the array aperture size, respectively, and SLL_{ref}, BW_{ref}, and SR_{th} being the sidelobe level, the beamwidth, and the sideband radiation threshold, respectively;
  (b) Setup of the PSO parameters, namely the inertial weight, w, the cognitive acceleration, C_1, the social acceleration, C_2, the number of swarm particles, S, the maximum number of iterations, K, and the convergence threshold, η_{th};

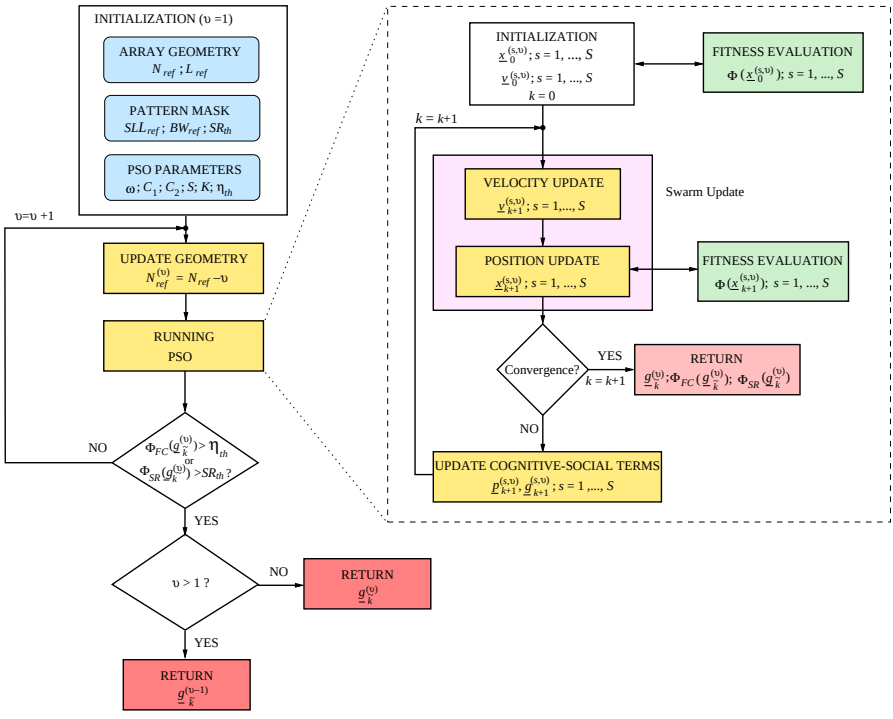

Figure 1. Flowchart of iterative PSO-based optimization procedure.

- **Step 2** — *Iterative Process*:
  (a) Update the number of array elements ($N_{ref}^{(\upsilon)} \leftarrow N_{ref} - \upsilon$);
  (b) Set the range of the variations of the problem degrees-of-freedom ($d^{\min} \leq d_n \leq d^{\max}$ and $\tau^{\min} \leq \tau_n \leq \tau^{\max}$);
  (c) Run the PSO as shown in Fig. 1 to minimize the following cost function taking into account the problem requirements and constraints:

$$\Phi\left(\underline{\tau}, \underline{d}\right) = \alpha_{CF}\Phi_{CF}\left(\underline{\tau}, \underline{d}\right) + \alpha_{SR}\Phi_{SR}\left(\underline{\tau}, \underline{d}\right) + \alpha_{L}\Phi_{L}\left(\underline{\tau}, \underline{d}\right) \quad (9)$$

  where $\Phi_{CF}(\underline{\tau}, \underline{d}) = \{\frac{\left|SLL_{ref} - SLL(\underline{\tau}, \underline{d})\right|^2}{\left|SLL_{ref}\right|^2} H[SLL(\underline{\tau}, \underline{d}) - SLL_{ref}] + \frac{|BW_{ref} - BW(\underline{\tau}, \underline{d})|^2}{|BW_{ref}|^2} H[BW(\underline{\tau}, \underline{d}) - BW_{ref}]\}$, $\Phi_{SR}(\underline{\tau}, \underline{d}) = \frac{P_{SR}(\underline{\tau}, \underline{d})}{P_{tot}(\underline{\tau}, \underline{d})}$, and $\Phi_{L}(\underline{\tau}, \underline{d}) = H[L(\underline{\tau}, \underline{d}) - L_{ref}]$, $H[\cdot]$ being the Heaviside step function. Moreover, α_{CF}, α_{SR}, and α_{L} are real positive weighting coefficients. In the PSO, the classical velocity and position update equations, respectively defined as [31]

$$v_{n,k+1}^{(s,\upsilon)} = w v_{n,k}^{(s,\upsilon)} + C_1 r_1 \left(p_{n,k}^{(s,\upsilon)} - x_{n,k}^{(s,\upsilon)}\right) + C_2 r_2 \left(g_{n,k}^{(\upsilon)} - x_{n,k}^{(s,\upsilon)}\right) \quad (10)$$

  and

$$\underline{x}_{k+1}^{(s,\upsilon)} = \underline{x}_{k}^{(s,\upsilon)} + \underline{v}_{k+1}^{(s,\upsilon)} \quad (11)$$

  are implemented, where $s = 1, \ldots, S$ and $\underline{x} = \{\underline{\tau}, \underline{d}\}$. In (10), r_1 and r_2 are two random variables having uniform distribution in the range [0, 1]. Moreover, $\underline{p}_k^{(s,\upsilon)} = \arg\{\min_{i=1,\ldots,k}[\Phi(\underline{x}_i^{(s,\upsilon)})]\}$, $s = 1, \ldots, S$, and $\underline{g}_k^{(\upsilon)} = \arg\{\min_{i=1,\ldots,k;;\, s=1,\ldots,S}[\Phi(\underline{x}_i^{(s,\upsilon)})]\}$ are the personal and global best solutions at the k-th PSO iteration, respectively [31];
- **Step 3** — *Stopping Criterion*:
  If $\{\Phi_{CF}(\underline{\tau}^{(\upsilon)}, \underline{d}^{(\upsilon)}) > \eta_{th}\}$ or $\{\Phi_{SR}(\underline{\tau}^{(\upsilon)}, \underline{d}^{(\upsilon)}) > SR_{th}\}$ and $\{\upsilon > 1\}$ then stop the iterative loop and return the solution $\underline{\tau}_{opt} = \underline{\tau}^{(\upsilon-1)}$ and $\underline{d}_{opt} = \underline{d}^{(\upsilon-1)}$. Otherwise, goto **Step 2** and increase the iteration index ($\upsilon \leftarrow \upsilon + 1$).

4. NUMERICAL VALIDATION

The first example of the numerical assessment is devoted to "describe" the proposed synthesis procedure. Towards this end, a Dolph-Chebyshev pattern with $SLL_{ref} = -25\,[\text{dB}]$ ($BW_{ref} = 8.51\,[\text{deg}]$) radiated by an array of $N_{ref} = 14$ isotropic elements has been considered as a representative reference case. While no constraints

have been chosen for the pulse durations (i.e., $\tau_n \in [\tau_{\min}; \tau_{\max}] = [0.0; 1.0]$), a restricted range $[0.40\lambda; 1.00\lambda]$ has been assumed for the inter-element array distances $d_n \in [d_{\min}; d_{\max}]$ to limit the mutual coupling effects. The upper bound for the sideband radiation has been also fixed to $SR_{th} = 10\%$. Concerning the optimization strategy, the calibration parameters of the PSO have been set to $w = 0.4$, $C_1 = 2.0$, $C_2 = 2.0$, $S = N_{ref}$, and $K = 2000$, while the cost function terms have been weighted as follows: $\alpha_{CF} = 10$, $\alpha_{SR} = 1$, and $\alpha_L = 10^3$ to prioritize the pattern matching at $h = 0$ keeping SLL and BW as close as possible to the reference one.

After completing *Step 3* at $\upsilon = 1$, the normalized pulse durations and the element positions turn out to be as in Fig. 2(a) affording the radiated beam patterns at the carrier frequency ($h = 0$) and the first two upper harmonic frequencies ($h = 1, 2$) shown in Fig. 2(b). The matching between the patterns synthesized at $h = 0$ with $N = 13$ elements and the reference one is almost perfect, the pattern features being $SLL_{PSO}^{\upsilon=1} = -25.02\,[\text{dB}]$ and $BW_{PSO}^{\upsilon=1} = 8.53\,[\text{deg}]$ (Table 1), while the sideband radiation turns out to be widely below the user-chosen threshold ($SR_{PSO}^{\upsilon=1} = 4.54\% < SR_{th} = 10\%$). Since the *Stopping Criterion* (Section 3) is not satisfied, the optimization loop is iterated by reducing the number of array elements. Table 1 summarizes the pattern features of the partial solutions synthesized at each υ-th iteration. As it can be noticed, there is a trade-off between the number of array elements (N) and the amount of wasted power (SR) for similar values of SLL, BW, and L. More specifically, the reduction of N causes an increase of SR. The final iteration is that at $\upsilon = 3$

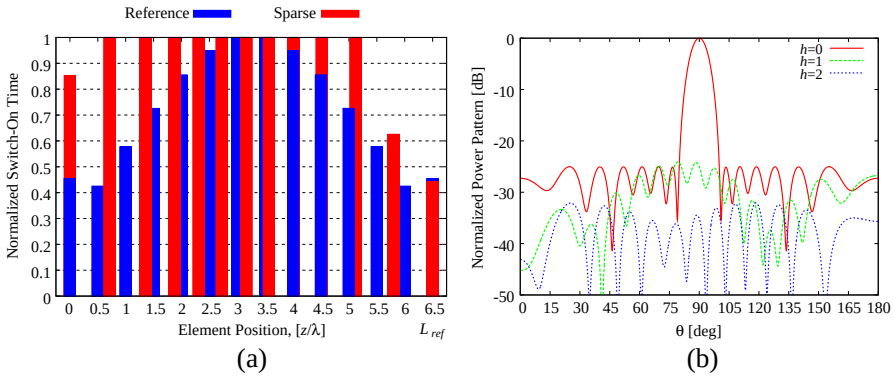

Figure 2. *Numerical assessment* — ($N_{ref} = 14$, $L_{ref} = 6.5\,\lambda$, $SLL_{ref} = -25\,\text{dB}$, $BW_{ref} = 8.51\,[\text{deg}]$) — $\upsilon = 1$ — (a) Optimized pulse sequences and (b) radiated power patterns ($h = 0$, 1, 2).

since the solution defined at $\upsilon = 4$ does not satisfy the project requirements in terms of sideband radiation (i.e., $SR_{PSO}^{\upsilon=4} = 14.96\%$) despite the good matching at the $h = 0$ ($SLL_{PSO}^{\upsilon=4} = -24.96\,[\text{dB}]$ and $BW_{PSO}^{\upsilon=4} = 8.51\,[\text{deg}]$, Table 1). The optimization result in terms of the duration of the periodic waveforms and the geometry of the array are reported in Fig. 3(a), whereas the radiated beam patterns are shown in Fig. 3(b). More in detail, Fig. 3(c) shows a comparison between the reference Dolph-Chebyshev pattern and the optimized one at the carrier frequency to assess the accuracy of the synthesis process. The efficiency of the optimization is also pointed out from the reduction of both the SR and the SBL. Indeed, the sideband radiation percentage and the sideband level decrease from $SR_{ref} = 22.22\%$ and $SBL_{ref} = -12.36\,[\text{dB}]$ down to $SR_{PSO}^{\upsilon=3} = 9.41\%$ and to $SBL_{PSO}^{\upsilon=3} = -19.52\,[\text{dB}]$, respectively. Fig. 4 details the SR

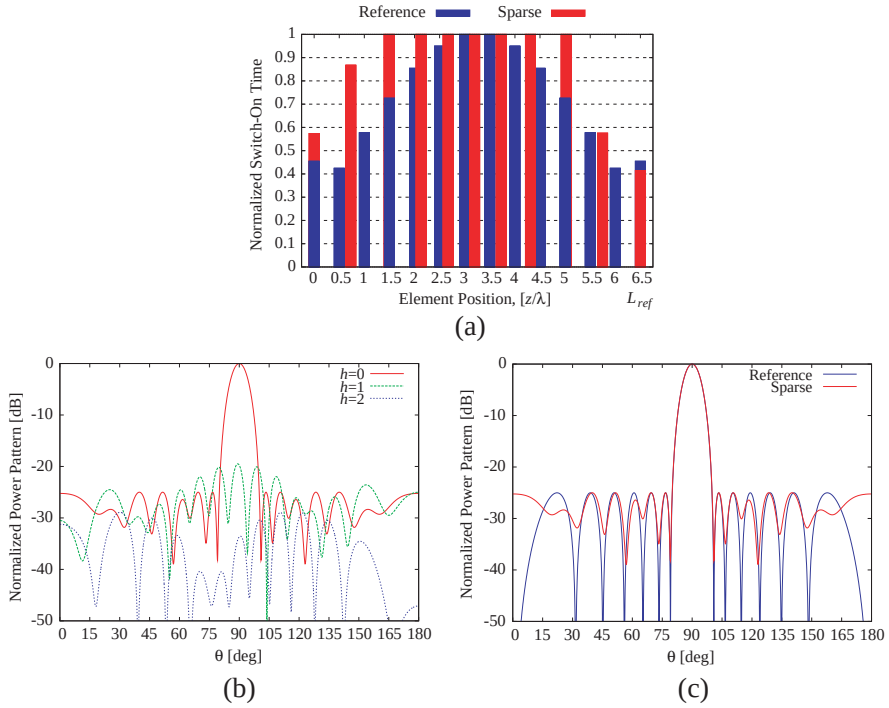

Figure 3. *Numerical assessment* — ($N_{ref} = 14$, $L_{ref} = 6.5\,\lambda$, $SLL_{ref} = -25\,\text{dB}$, $BW_{ref} = 8.51\,[\text{deg}]$) — $\upsilon = 3$ — (a) Optimized pulse sequences, (b) radiated power patterns ($h = 0, 1, 2$), and (c) comparison between optimized and reference pattern at $h = 0$.

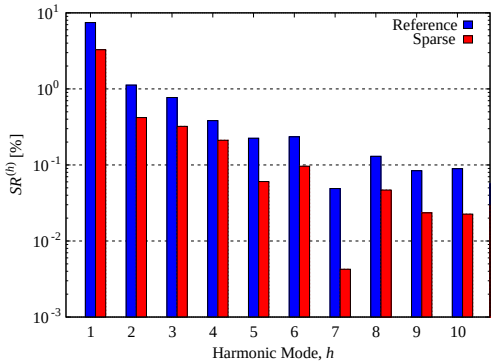

Figure 4. *Numerical assessment* — ($N_{ref} = 14$, $L_{ref} = 6.5\lambda$, $SLL_{ref} = -25\,\text{dB}$, $BW_{ref} = 8.51\,[\text{deg}]$) — $\upsilon = 3$ — optimized and reference harmonic sideband radiations.

Table 1. *Numerical assessment* — ($N_{ref} = 14$, $L_{ref} = 6.5\,\lambda$, $SLL_{ref} = -25\,\text{dB}$, $BW_{ref} = 8.51\,[\text{deg}]$) — pattern features.

	N	$L\,[\lambda]$	$SLL\,[\text{dB}]$	$BW\,[\text{deg}]$	$SBL\,[\text{dB}]$	$SR\,[\%]$
$Reference$	14	6.50	−25.00	8.51	−12.36	22.22
PSO, $\upsilon = 1$	13	6.50	−25.02	8.53	−24.09	4.54
PSO, $\upsilon = 2$	12	6.50	−25.00	8.52	−21.73	6.43
PSO, $\upsilon = 3$	11	6.50	−24.93	8.52	−19.52	9.41
PSO, $\upsilon = 4$	10	6.50	−24.96	8.51	−16.81	14.96

reduction with respect to the reference for each h-th term of the PSO optimized solution.

The second numerical experiment, referred as "*Case A*", considers as reference the array configuration from [9] and it is aimed at proving that, unlike [9] where only pulse durations have been optimized, the joint optimization of both pulse durations and array element locations allows one non-negligible improvements. With reference to the following optimization setup: $N_{ref} = 26$, $SLL_{ref} = -20\,[\text{dB}]$, $BW_{ref} = 2.9\,[\text{deg}]$, and $SR_{th} = 3.57\%$, the optimization process stops at the iteration $\upsilon = 5$ by returning the $\upsilon = 4$ solution corresponding to an array of $N_{PSO}^{\upsilon=4} = N_{opt} = 22$ elements whose geometry and temporal excitations are given in Fig. 5(a) affording the harmonic patterns at $h = 0, 1, 2$ displayed in Fig. 5(b). As it can be observed by the pattern behaviors in Fig. 5(c) and the values of the pattern features in Table 2, the synthesized solution fully satisfies the design requirements ($SLL_{PSO}^{\upsilon=4} = -20\,[\text{dB}]$ vs. $SLL_{ref} = -20\,[\text{dB}]$ and

$SR_{PSO}^{\upsilon=4} = 3.54\%$ vs. $SR_{thr} = 3.57\%$) except for a negligible difference in the beam width ($BW_{PSO}^{\upsilon=4} = 2.92\,[\text{deg}]$ vs. $BW_{ref} = 2.90\,[\text{deg}]$). Moreover, it is worth noticing the significant reduction of the array size ($L_{ref} = 19.6\,\lambda \rightarrow L_{PSO}^{\upsilon=4} = 18.17\,\lambda$ corresponding to an aperture reduction of $\Delta L = 7.3\,\%$ being $\Delta L \triangleq \frac{L_{ref} - L_{PSO}^{\upsilon=4}}{L_{ref}} \times 100$) as well as the number of radiating elements ($N_{ref} = 26 \rightarrow N_{PSO}^{\upsilon=4} = 22$ equivalent to an element saving of about $\Delta N = 15.4\%$ being $\Delta N \triangleq \frac{N_{ref} - N_{PSO}^{\upsilon=4}}{N_{ref}} \times 100$).

The third example ("*Case B*") is devoted to compare a solution obtained with the proposed *PSO*-based approach with a result synthesized by means of the *DE* in [22] that is considered as reference one. In [22], the design of sparse *TMA*s is addressed by controlling the losses in the *SR* through the minimization of the *SBL* for the first harmonic term ($h = 1$). The element locations and the pulse

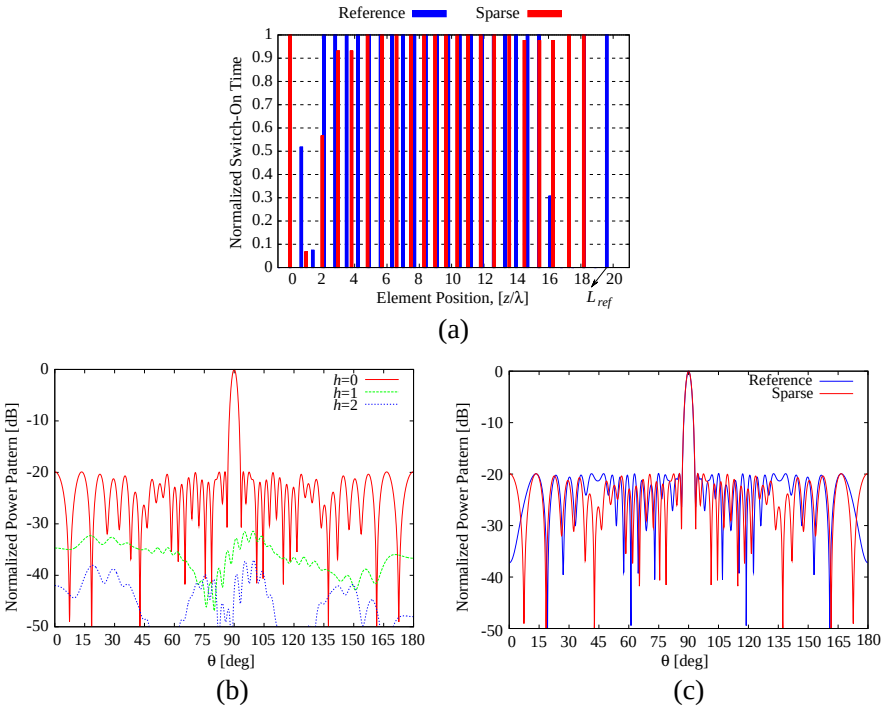

Figure 5. *Comparative study "Case A"* — ($N_{ref} = 26$, $L_{ref} = 19.6\,\lambda$, $SLL_{ref} = -20\,\text{dB}$, $BW_{ref} = 2.90\,[\text{deg}]$) — $\upsilon = 4$ — (a) Optimized pulse sequences, (b) radiated power patterns ($h = 0, 1, 2$), and (c) comparison between optimized and reference pattern at $h = 0$.

sequence achieved with the DE and PSO ($\upsilon = 1$) are shown in Fig. 6(a). Although the number of radiating elements is the same ($N_{ref} = N_{PSO}^{\upsilon=1} = 32$), the array synthesized by means of the proposed method requires a narrower aperture ($L_{ref} = 23.8\,\lambda \rightarrow L_{PSO}^{\upsilon=1} = 23.5\,\lambda$) with a reduction of $\Delta L = 2.1\%$. The corresponding power patterns generated at the central frequency ($h = 0$) are shown in Fig. 6(b) and the pattern features are reported in Table 3. The two beams are characterized by approximately the same sidelobe behavior ($SLL_{Ref} = -29.80\,[\text{dB}]$ vs. $SLL_{PSO}^{\upsilon=1} = -29.75\,[\text{dB}]$) and mainlobe ($BW_{Ref} = 2.70\,[\text{deg}]$ vs. $BW_{PSO}^{\upsilon=1} = 2.72\,[\text{deg}]$). As for the sideband radiations (Fig. 7), the power losses are more than 1% lower for the PSO solution ($SR_{Ref} = 9.68\%$ vs. $SR_{PSO}^{\upsilon=1} = 8.45\%$) although the DE solution has a lower sideband level [$SBL_{Ref} = -22.70\,[\text{dB}]$ vs. $SBL_{PSO}^{\upsilon=1} = -22.35\,[\text{dB}]$ — Fig. 7(a)]. Since the maximum SBL may also appear at higher harmonics, the minimization of the total power loss turns out being more effective for SR rejection than the minimization of the SBL only.

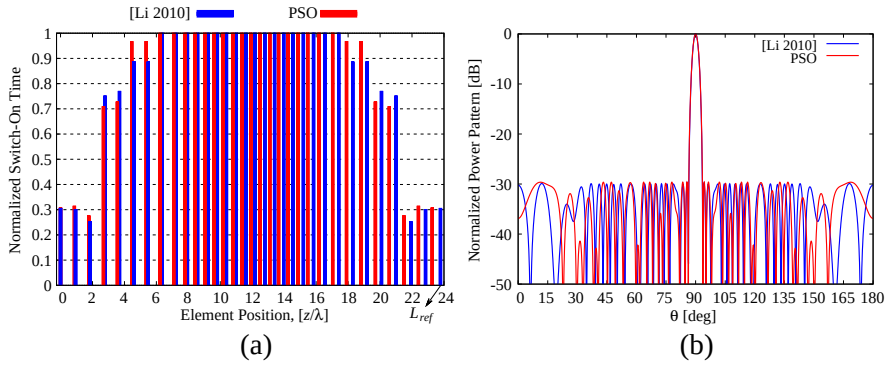

Figure 6. *Comparative study "Case B"* — ($N_{ref} = 32$, $L_{ref} = 23.78\lambda$, $SLL_{ref} = -29.8\,\text{dB}$, $BW_{ref} = 2.70\,[\text{deg}]$) — $\upsilon = 1$ — (a) Optimized pulse sequences and (b) radiated power patterns ($h = 0$) obtained with the proposed iterative PSO approach and the DE [22].

Table 2. *Comparative study "Case A"* — ($N_{ref} = 26$, $L_{ref} = 19.6\,\lambda$, $SLL_{ref} = -20\,\text{dB}$, $BW_{ref} = 2.90\,[\text{deg}]$) — pattern features.

	N	$L\,[\lambda]$	$SLL\,[\text{dB}]$	$BW\,[\text{deg}]$	$SBL\,[\text{dB}]$	$SR\,[\%]$
[*Poli* 2010]	30	20.30	−20.00	2.84	−28.91	3.57
PSO, $\upsilon = 4$	22	18.17	−20.00	2.92	−31.47	3.54

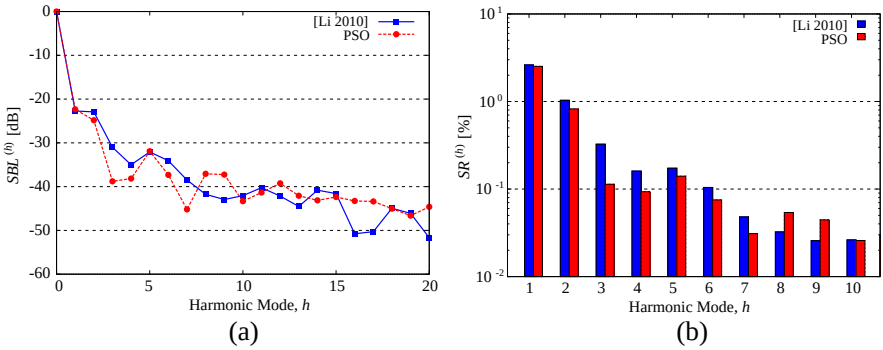

Figure 7. *Comparative study "Case B"* — ($N_{ref} = 32$, $L_{ref} = 23.78\,\lambda$, $SLL_{ref} = -29.8\,\text{dB}$, $BW_{ref} = 2.70\,[\text{deg}]$) — $\upsilon = 1$ — (a) Behaviors of the sideband level and (b) sideband radiation versus the harmonic order h.

Table 3. *Comparative study "Case B"* — ($N_{ref} = 32$, $L_{ref} = 23.78\,\lambda$, $SLL_{ref} = -29.8\,\text{dB}$, $BW_{ref} = 2.70\,[\text{deg}]$) — pattern features.

	N	$L\,[\lambda]$	$SLL\,[\text{dB}]$	$BW\,[\text{deg}]$	$SBL\,[\text{dB}]$	$SR\,[\%]$
$[Li\,2010]$	32	23.8	−29.80	2.70	−22.70	9.68
PSO, $\upsilon = 1$	32	23.3	−29.75	2.72	−22.35	8.45

The fourth numerical example ("*Case C*") is aimed at comparing the results from the proposed approach with those coming from the hybrid multi-stage optimization strategy based on convex programming (CP) and simulated annealing [23]. Unlike [23], the algorithm in Section 3 does not contemplate the optimization of the switch-on instants to suppress the sideband level since we are interested at the minimization of sideband power, while modifying $\underline{\tau}^{rise} = \{\tau_n^{rise};\, n = 0, \ldots, N_{opt} - 1\}$ could increases it when the inter-element spacing differs from $d_n = 0.5\lambda$, $n = 1, \ldots, N-1$. However, for a fair comparison, an additional step (*Step 4*) has been added to the optimization procedure consisting in the PSO-based minimization of the following cost function [23]:

$$\Phi^{(k)}\left(\underline{\tau}^{rise}\right) = SBL^{(k)}\left(\underline{\tau}^{rise}\right), \tag{12}$$

once element positions and pulse durations have been set through *Step 3*.

The benchmark configuration has been chosen equal to a Dolph-Chebyshev pattern with $BW_{ref} = 7.95\,[\text{deg}]$ radiated by an array of $N_{ref} = 16$ time-modulated elements, while the sideband radiation

threshold has been fixed to $SR_{th} = 20.03\%$ [23]. By taking into account the symmetry of the pulse durations with respect to the center of the array as in [23]), the optimal solution $\upsilon = 2$ described in terms of the pulse sequences and the radiated beam patterns in Fig. 8(a) and Fig. 8(b), respectively, has been yielded. After completing also the *Step 4* (12), the final result turned out as that shown in Fig. 9(a) radiating the beam pattern in Fig. 9(b). Such an optimized solution

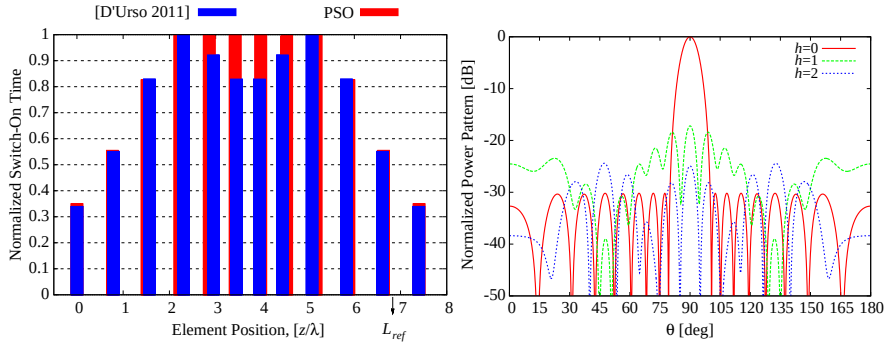

Figure 8. *Comparative study "Case C"* — ($N_{ref} = 16$, $L_{ref} = 7.4\,\lambda$, $SLL_{ref} = -30\,\mathrm{dB}$, $BW_{ref} = 7.95\,[\mathrm{deg}]$) — $\upsilon = 2$ (*Step 3*) — (a) Optimized pulse sequences and (b) radiated power patterns ($h = 0, 1, 2$).

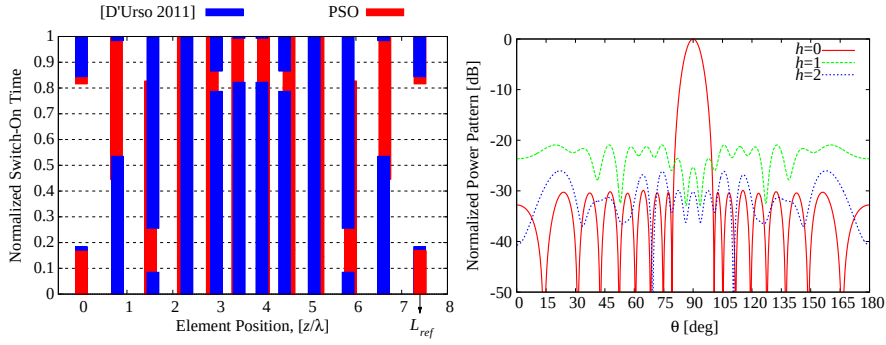

Figure 9. *Comparative study "Case C"* — ($N_{ref} = 16$, $L_{ref} = 7.4\,\lambda$, $SLL_{ref} = -30\,\mathrm{dB}$, $BW_{ref} = 7.95\,[\mathrm{deg}]$) — $\upsilon = 2$ (*Step 4*) — (a) Optimized pulse sequences and (b) radiated power patterns ($h = 0,\ 1,\ 2$).

is characterized by a lower sideband level ($SBL_{PSO}^{v=2} = -20.94\,[\text{dB}]$ vs. $SBL_{CP-SA}^{Stage\,2} = -19.87\,[\text{dB}]$ — Table 4) and an improvement of the SR [Fig. 10(b)] as well as a better behavior of the sideband level of the higher-order harmonics [Fig. 10(a)] with an average reduction of $\Delta SBL = 4.1\,[\text{dB}]$. For completeness, the pattern parameters about reference and optimized pattern/geometry are reported in Table 4. As expected, the pulse shifting causes an increasing of the percentage of sideband radiation over the total radiated power ($SR_{PSO}^{v=2-Step\,3} = 13.18\%$ vs. $SR_{PSO}^{v=2-Step\,4} = 16.90\%$) although to a value smaller than that in [23] ($SR_{PSO}^{v=2-Step\,4} = 16.90\%$ vs. $SR_{CP-SA}^{Stage\,2} = 22.91\%$).

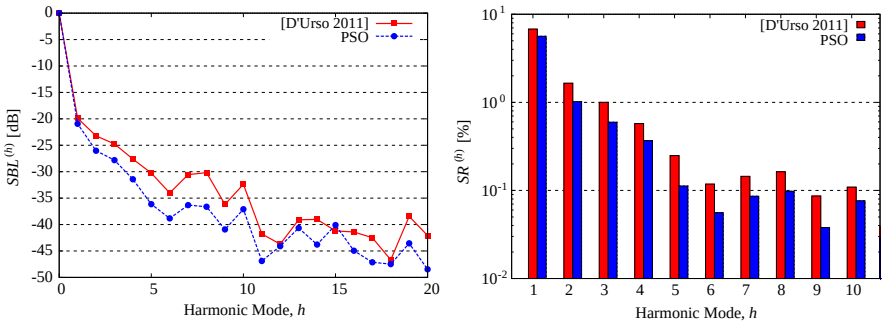

Figure 10. *Comparative study "Case C"* — ($N_{ref} = 16$, $L_{ref} = 7.4\,\lambda$, $SLL_{ref} = -30\,\text{dB}$, $BW_{ref} = 7.95\,[\text{deg}]$) — (a) Behaviors of the sideband level and (b) sideband radiation versus the harmonic order h.

Table 4. *Comparative study "Case C"* — ($N_{ref} = 16$, $L_{ref} = 7.4\,\lambda$, $SLL_{ref} = -30\,\text{dB}$, $BW_{ref} = 7.95\,[\text{deg}]$) — pattern features.

	N	$L\,[\lambda]$	$SLL\,[\text{dB}]$	$BW\,[\text{deg}]$	$SBL\,[\text{dB}]$	$SR\,[\%]$
[*D'Urso* 2011], Stage-1	12	7.40	−30.00	7.95	−15.06	20.03
[*D'Urso* 2011], Stage-2	12	7.40	−30.00	7.95	−19.87	22.91
PSO, $v = 2$, Step-3	12	7.40	−29.95	7.95	−17.19	13.81
PSO, $v = 2$, Step-4	12	7.40	−29.95	7.95	−20.94	16.90

5. CONCLUSIONS

In this paper, a strategy for the synthesis of sparse *TMA*s has been presented. Starting from a reference array and a reference pattern, the procedure iteratively reduce the number of array elements and execute an optimization aimed at minimizing the mismatching with the reference at the carrier frequency while limiting the amount of sideband power. The set of numerical experiments results have pointed out the following main items:

- There is a trade-off between antenna performance, number of array elements, and amount of sideband radiation and the sideband radiation threshold strongly impacts on the array sparsening;
- The exploitation of sparse geometries as additional degrees-of-freedom allows one to improve the synthesized solutions. More specifically, the number of array elements can be significantly reduced whether element positions can be arbitrarily located within the array aperture still keeping equal pattern features (i.e., SLL, BW, and SR).

Future lines of research will extend the proposed approach towards planar and conformal array architectures.

REFERENCES

1. Shanks, H. E. and R. W. Bickmore, "Four-dimensional electromagnetic radiators," *Canad. J. Phys.*, Vol. 37, 263–275, 1959.
2. Labate, M. G., A. Buonanno, M. D'Urso, G. Calzolaio, A. Vacca, L. Zeni, G. Leone, and G. Roccardo, "Photoconductive switches for radar systems exploiting time domain," *Proc. 5th European Conference on Antennas and Propagation (EuCAP 2011)*, 850–852, Rome, Italy, Apr. 11–15, 2011.
3. Kummer, W. H., A. T. Villeneuve, T. S. Fong, and F. G. Terrio, "Ultra-low sidelobes from time-modulated arrays," *IEEE Trans. Antennas Propag.*, Vol. 11, No. 6, 633–639, 1963.
4. Yang, S., Y. B. Gan, and A. Qing, "Sideband suppression in time-modulated linear arrays by the differential evolution algorithm," *IEEE Antennas Wireless Propag. Lett.*, Vol. 1, No. 1, 173–175, 2002.
5. Yang, S., Y. B. Gan, and P. K. Tan, "Comparative study of low sidelobe time modulated linear arrays with different time schemes," *Journal of Electromagnetic Waves and Applications*, Vol. 18, No. 11, 1443–1458, 2004.

6. Mandal, S. K., G. K. Mahanti, and R. Ghatak, "Differential evolution algorithm for optimizing the conflicting parameters in time-modulated linear array antennas," *Progress In Electromagnetics Research B*, Vol. 51, 101–118, 2013.
7. Zhu, Q., S. Yang, R. Yao, and Z. Nie, "Design of a low sidelobe 4D planar array including mutual coupling," *Progress In Electromagnetics Research M*, Vol. 31, 103–116, 2013.
8. Fondevila, J., J. C. Brégains, F. Ares, and E. Moreno, "Optimizing uniformly excited linear arrays through time modulation," *IEEE Antennas Wireless Propag. Lett.*, Vol. 3, No. 1, 298–301, 2004.
9. Poli, L., P. Rocca, L. Manica, and A. Massa, "Handling sideband radiations in time-modulated arrays through particle swarm optimization," *IEEE Trans. Antennas Propag.*, Vol. 58, No. 4, 1408–1411, Apr. 2010.
10. Poli, L., P. Rocca, L. Manica, and A. Massa, "Time modulated planar arrays — Analysis and optimisation of the sideband radiations," *IET Microw. Antennas Propag.*, Vol. 4, No. 9, 1165–1171, 2010.
11. Rocca, P., L. Poli, G. Oliveri, and A. Massa, "Synthesis of time-modulated planar array with controlled harmonic radiations," *Journal of Electromagnetic Waves and Applications*, Vol. 24, No. 4, 827–838, 2010.
12. Poli, L., P. Rocca, L. Manica, and A. Massa, "Pattern synthesis in time-modulated linear arrays through pulse shifting," *IET Microw. Antennas Propag.*, Vol. 4, No. 9, 1157–1164, 2010.
13. Yang, S., Y. B. Gan, A. Qing, and P. K. Tan, "Design of a uniform amplitude time modulated linear array with optimized time sequences," *IEEE Trans. Antennas Propag.*, Vol. 53, No. 7, 2337–2339, Jul. 2005.
14. Zhu, Q., S. Yang, L. Zheng, and Z. Nie, "Design of a low sidelobe time modulated linear array with uniform amplitude and sub-sectional optimized time-steps," *IEEE Trans. Antennas Propag.* Vol. 60, No. 9, 4436–4439, Sep. 2012.
15. Bekele, E. T., L. Poli, M. D'Urso, P. Rocca, and A. Massa, "Pulse-shaping strategy for time modulated arrays — Analysis and design," *IEEE Trans. Antennas Propag.*, Vol. 61, No. 7, 3525–3537, Jul. 2013.
16. Tong, Y. and A. Tennant, "Sideband level suppression in time-modulated linear arrays using modified switching sequences and fixed bandwidth elements," *Elect. Lett.*, Vol. 48, No. 1, 10–11, Jan. 2012.

17. Poli, L., P. Rocca, and A. Massa, "Sideband radiation reduction exploiting pattern multiplication in directive time-modulated linear arrays," *IET Microw. Antennas Propag.*, Vol. 6, No. 2, 214–222, 2012.
18. Aksoy, E. and E. Afacan, "Thinned nonuniform amplitude time-modulated linear arrays," *IEEE Antennas Wireless Propag. Lett.*, Vol. 9, 514–517, May 2010.
19. Chen, Y., S. Yang, and Z. Nie, "Synthesis of satellite footprint patterns from time-modulated planar arrays with very low dynamic range ratios," *Int. J. Numer. Model.*, Vol. 21, 493–506, 2008.
20. Rocca, P., L. Manica, L. Poli, and A. Massa, "Synthesis of compromise sum-difference arrays through time-modulation," *IET Radar Sonar Navig.*, Vol. 3, No. 6, 630–637, Nov. 2009.
21. Rocca, P., L. Poli, G. Oliveri, and A. Massa, "Synthesis of sub-arrayed time modulated linear arrays through a multi-stage approach," *IEEE Trans. Antennas Propag.*, Vol. 59, No. 9, 3246–3254, Sep. 2011.
22. Li, G., S. Yang, M. Huang, and Z. Nie, "Sidelobe suppression in time modulated linear arrays with unequal element spacing," *Journal of Electromagnetic Waves and Applications*, Vol. 24, Nos. 5–6, 775–783, 2010.
23. D'Urso, M., A. Iacono, A. Iodice, and G. Franceschetti, "Optimizing uniformly excited time-modulated linear arrays," *Proc. 5th European Conference on Antennas and Propagation (EUCAP 2011)*, 2082–2086, Rome, Italy, Apr. 11–15, 2011.
24. Liu, Y., Z. Nie, and Q. H. Liu, "Reducing the number of antenna elements in a linear antenna array by the matrix pencil method," *IEEE Trans. Antennas Propag.*, Vol. 56, No. 9, 2955–2962, Sep. 2008.
25. Oliveri, G. and A. Massa, "Bayesian compressive sampling for pattern synthesis with maximally sparse non-uniform linear arrays," *IEEE Trans. Antennas Propag.*, Vol. 59, No. 2, 467–481, Feb. 2011.
26. Oliveri, G., M. Carlin, and A. Massa, "Complex-weight sparse linear array synthesis by Bayesian compressive sampling," *IEEE Trans. Antennas Propag.*, Vol. 60, No. 5, 2309–2326, May 2012.
27. Viani, F., G. Oliveri, and A. Massa, "Compressive sensing pattern matching techniques for synthesizing planar sparse arrays," *IEEE Trans. Antennas Propag.*, Vol. 61, No. 9, 4577–4587, Sep. 2013.

28. Prisco, G. and M. D'Urso, "Maximally sparse arrays via sequential convex optimization," *IEEE Antennas Wireless Propag. Lett.*, Vol. 11, 192–195, 2012.
29. Fuchs, B., "Synthesis of sparse arrays with focused or shaped beam pattern via sequential convex optimizations," *IEEE Trans. Antennas Propag.*, Vol. 60, No. 7, 3499–3503, Jul. 2012.
30. Poli, L., P. Rocca, M. D'Urso, and A. Massa, "Optimized design of sparse time-modulated linear arrays," *Proc. 7th European Conference in Antennas and Propagation (EuCAP 2013)*, 138–141, Gothenburg, Sweden, Apr. 8–12, 2013.
31. Rocca, P., M. Benedetti, M. Donelli, D. Franceschini, and A. Massa, "Evolutionary optimization as applied to inverse scattering problems," *Inv. Prob.*, Vol. 24, 1–41, Invited Topical Review Paper, 2009.
32. Brégains, J. C., J. Fondevila, G. Franceschetti, and F. Ares, "Signal radiation and power losses of time-modulated arrays," *IEEE Trans. Antennas Propag.*, Vol. 56, No. 6, 1799–1804, Jun. 2008.
33. Aksoy, E. and E. Afacan, "Calculation of sideband power radiation in time-modulated arrays with asymmetrically positioned pulses," *IEEE Antennas and Wireless Propag. Lett.*, Vol. 11, 133–136, 2012.